Article

Synthesis, Characterization, and Computational Studies of 6-(RR#N)-*nido*-5,7-CBH: A Polyborane Cluster with a Cage-Boron Having an Exopolyhedral Dative Boron#Nitrogen Double Bond

Yuqi Li, and Larry G. Sneddon

J. Am. Chem. Soc., **2008**, 130 (34), 11494-11502 • DOI: 10.1021/ja803297b • Publication Date (Web): 05 August 2008

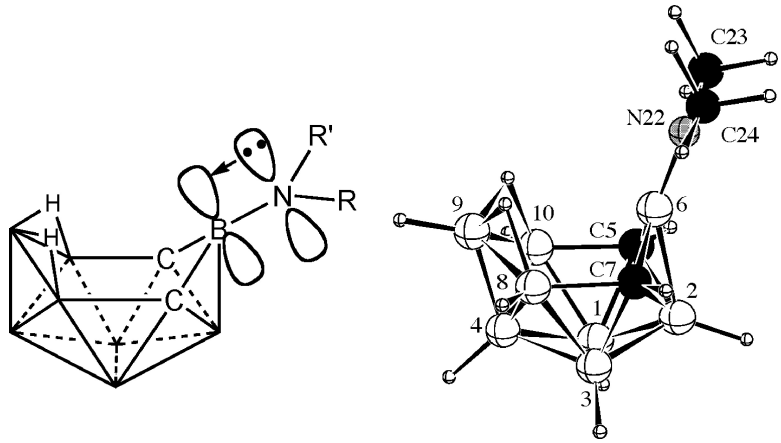

More About This Article

Additional resources and features associated with this article are available within the HTML version:

- Supporting Information
- Access to high resolution figures
- Links to articles and content related to this article
- Copyright permission to reproduce figures and/or text from this article

View the Full Text HTML

J|A|C|S
ARTICLES

Published on Web 08/05/2008

Synthesis, Characterization, and Computational Studies of 6-(RR′N)-*nido*-5,7-$C_2B_8H_{11}$: A Polyborane Cluster with a Cage-Boron Having an Exopolyhedral Dative Boron−Nitrogen Double Bond

Yuqi Li and Larry G. Sneddon*

Department of Chemistry, University of Pennsylvania, Philadelphia, Pennsylvania 19104-6323

Received May 3, 2008; E-mail: lsneddon@sas.upenn.edu

Abstract: The reactions of the *arachno*-4,6-$C_2B_7H_{13}$ carborane with the secondary and primary amines, Me_2NHBH_3 and $^tBuNH_2BH_3$, in ionic liquid media result in both boron-insertion into the cage at a position across the two cage-carbons and additional hydrogen-elimination via the reaction of a hydridic B−H with a protonic amine N−H hydrogen to produce the 6-(RR′N)-*nido*-5,7-$C_2B_8H_{11}$ carboranes. Computational characterizations of these compounds and the previously reported 6-ClC_6H_4-9-(RR′N)-*nido*-6-NB_9H_{10} azaboranes indicate that the amine-nitrogens form unique exopolyhedral dative B═N double bonds with a cage-boron.

Introduction

As part of our interest in the activating effects of ionic liquid media[1] for polyborane reactions, we have been investigating ionic-liquid-based polyborane cage-growth reactions. As shown in the examples in eqs 1,[2] 2,[3] and 3,[4] thermally induced reactions of polyhedral boranes, heteroboranes, and carboranes with amine borane adducts have previously been employed as one route to cage-expanded clusters.

$$\textit{nido}\text{-}B_{10}H_{14} + 2Et_3NBH_3 \xrightarrow{\Delta} [Et_3NH^+]_2[\textit{closo}\text{-}B_{12}H_{12}]^{2-} + 3H_2 \quad (1)$$

$$\textit{arachno}\text{-9-L-6-}SB_9H_{11} + Et_3NBH_3 \xrightarrow{\Delta} [Et_3NH^+][\textit{nido}\text{-}SB_{10}H_{11}]^- + H_2 + L \quad (2)$$

$$\textit{nido}\text{-2,3-}Et_2C_2B_4H_6 + Et_3NBH_3 \xrightarrow{\Delta} \textit{closo}\text{-2,3-}Et_2C_2B_5H_5 + 2\,H_2 + Et_3N \quad (3)$$

We report here that while the *arachno*-4,6-$C_2B_7H_{13}$ carborane undergoes an analogous cage-expansion to produce *closo*-1,6-$C_2B_8H_{10}$ when reacted with Me_3NBH_3 in 1-butyl-3-methylimidazolium chloride (bmimCl) ionic liquid solvent, its reactions with the secondary and primary amines, Me_2NHBH_3 and $^tBuNH_2BH_3$, proceed quite differently, resulting in both boron-insertion into the cage and hydrogen-elimination via the reaction of a hydridic cage B−H with an amine protonic N−H hydrogen to produce the 6-(RR′N)-*nido*-5,7-$C_2B_8H_{11}$ carboranes in which the nitrogen forms a unique exopolyhedral dative B═N double bond with the B6 cage boron.

Experimental Section

General Synthetic Procedures and Materials. Unless otherwise noted, all reactions and manipulations were performed in dry glassware under nitrogen or argon atmospheres using the high vacuum or inert-atmosphere techniques described by Shriver.[5]

The 1-butyl-3-methylimidazolium chloride (bmimCl) (Fluka) was dried by carrying out an azeotropic distillation with toluene followed by in vacuo drying, then stored in the dry box. The *arachno*-4,6-$C_2B_7H_{13}$ was prepared according to the literature procedure.[6] HCl·diethyl ether solution (1 M), trimethylamine borane, dimethylamine borane, and *tert*-butylamine borane (Aldrich) were used as received. $CDCl_3$ (Cambridge Isotope Laboratory) was used as received.

Physical Measurements. ^{1}H NMR at 400.1 MHz and ^{11}B NMR spectra at 128.4 MHz were obtained on a Bruker DMX 400 spectrometer. All ^{11}B NMR chemical shifts are referenced to external $BF_3{\cdot}O(C_2H_5)_2$ (0.00 ppm) with a negative sign indicating an upfield shift. All ^{1}H chemical shifts were measured relative to residual protons in the $CDCl_3$ lock solvent (7.27 ppm) and are referenced to Me_4Si (0.00 ppm). High and low resolution mass spectra (HRMS and LRMS) using negative chemical ionization (NCI) techniques were recorded on a Micromass Autospec spectrometer.

Reaction of *arachno*-4,6-$C_2B_7H_{13}$ and Trimethylamine Borane in the Absence of an Ionic Liquid. A 50 mL 2-neck round-bottom flask equipped with a septum, stir bar, and vacuum adapter was charged under an inert atmosphere with 0.191 g (1.65 mmol) of *arachno*-4,6-$C_2B_7H_{13}$, 0.353 g (4.84 mmol) of trimethylamine borane, and ∼10 mL of toluene. After heating the reaction mixture in a 120 °C oil bath for 1 h, analysis by ^{11}B NMR of an

(1) (a) Kusari, U.; Li, Y.; Bradley, M. G.; Sneddon, L. G. *J. Am. Chem. Soc.* **2004**, *126*, 8662–8663. (b) Li, Y.; Kusari, U.; Carroll, P. J.; Bradley, M. G.; Sneddon, L. G. *Pure Appl. Chem.* **2006**, *78*, 1349–1355. (c) Bluhm, M. E.; Bradley, M. G.; Butterick, R. III; Kusari, U.; Sneddon, L. G. *J. Am. Chem. Soc.* **2006**, *128*, 7748–7749.
(2) Miller, H. C.; Muetterties, E. L. *Inorg. Synth.* **1967**, *10*, 88–91.
(3) Hertler, W. R.; Klanberg, F.; Mutterties, E. L. *Inorg. Chem.* **1967**, *6*, 1696–1706.
(4) (a) Beck, J. S.; Kahn, A. P.; Sneddon, L. G. *Organometallics* **1986**, *5*, 2552–2553. (b) Beck, J. S.; Sneddon, L. G. *Inorg. Chem.* **1990**, *29*, 295–302.
(5) Shriver, D. F.; Drezdzon, M. A. *The Manipulation of Air-Sensitive Compounds*; 2nd ed., Wiley: New York, 1986.
(6) Garrett, P. M.; George, T. A.; Hawthorne, M. F. *Inorg. Chem.* **1969**, *8*, 2008–2009.

10.1021/ja803297b CCC: $40.75

aliquot of the toluene layer showed only unreacted *arachno*-4,6-$C_2B_7H_{13}$ and trimethylamine borane.

Reaction of *arachno*-4,6-$C_2B_7H_{13}$ and Dimethylamine Borane in the Absence of an Ionic Liquid. A 50 mL 2-neck round-bottom flask equipped with a septum, stir bar, and vacuum adapter was charged under an inert atmosphere with 0.195 g (1.73 mmol) of *arachno*-4,6-$C_2B_7H_{13}$, 0.382 g (6.48 mmol) of dimethylamine borane, and ~10 mL of toluene. After heating the reaction mixture in a 120 °C oil bath for 1 h, analysis by ^{11}B NMR of an aliquot of the toluene layer showed only unreacted *arachno*-4,6-$C_2B_7H_{13}$ and dimethylamine borane.

***closo*-1,6-$C_2B_8H_{10}$ (1).** Analysis by ^{11}B NMR of an aliquot of the toluene layer following the reaction of 0.196 g (1.74 mmol) of *arachno*-4,6-$C_2B_7H_{13}$ and 0.312 g (4.28 mmol) of trimethylamine borane in biphasic toluene (~10 mL)/bmimCl (0.183 g, 1.05 mmol) at 120 °C for ~3 h showed the formation of only *closo*-1,6-$C_2B_8H_{10}$ (**1**).[7]

6-(Me_2N)-*nido*-5,7-$C_2B_8H_{11}$ (2). Analysis by ^{11}B NMR of an aliquot of the toluene layer following the reaction of 0.228 g (2.02 mmol) of *arachno*-4,6-$C_2B_7H_{13}$ and 0.305 g (5.18 mmol) of dimethylamine borane in biphasic toluene (~10 mL)/bmimCl (0.180 g, 1.03 mmol) at 120 °C for ~3 h showed the formation of 6-(Me_2N)-*nido*-5,7-$C_2B_8H_{11}$ (**2**) and *closo*-1,6-$C_2B_8H_{10}$ (**1**). The toluene layer was separated by pipet, and then the toluene and **1** were removed in vacuo to leave behind **2** as an air-sensitive liquid. **2** was obtained in comparable crude yields as **3** (>~50%) below, but decomposed much more readily. As a result, it was not possible to sufficiently separate **2** from organic impurities, such that reliable ^{1}H NMR and IR spectra could be obtained. For **2**, NCI-LRMS (*m/e*) calcd for $^{12}C_4{}^{11}B_8{}^1H_{17}{}^{14}N^-$, 167; found, 167. ^{11}B NMR (128.4 MHz, $CDCl_3$, ppm, J = Hz): 22.7 (s, 1B), −3.9 (d, 2B, J 152), −6.2 (d, 1B, J 176), −25.8 (d, 2B, J 168), −36.5 (d, 1B, J 204), −45.1 (d, 1B, J 153).

6-(^{t}BuHN)-*nido*-5,7-$C_2B_8H_{11}$ (3). Reaction of 0.226 g (2.00 mmol) of *arachno*-4,6-$C_2B_7H_{13}$ and 0.334 g (3.84 mmol) of *tert*-butylamine borane in biphasic toluene (~10 mL)/bmimCl (0.123 g, 0.70 mmol) at 120 °C for ~3 h, gave 6-(^{t}BuHN)-*nido*-5,7-$C_2B_8H_{11}$ (**3**) and *closo*-1,6-$C_2B_8H_{10}$ (**1**). The toluene layer was separated by pipet, and then the toluene and **1** were removed in vacuo to leave behind 0.196 g (1.01 mmol, 71% yield) of **3** as an air-sensitive oily white solid that always contained small amounts of BH_4^- impurity. For **3**, NCI-HRMS (*m/e*) calcd for $^{12}C_6{}^{11}B_8{}^1H_{20}{}^{14}N^-$ (M − H), 194.2340; found, 194.2340. ^{11}B NMR (128.4 MHz, $CDCl_3$, ppm, J = Hz): 22.5 (s, 1B), −3.8 (d, 2B, J 150), −6.5 (d, 1B, J 173), −25.1 (d, 1B, J 170), −27.2 (d, 1B, J 130), −36.4 (d, 1B J 140), −45.1 (d, 1B, J 148). ^{1}H NMR (400.1 MHz, $CDCl_3$, ppm): 1.38 (s, cage-CH), 1.20 (s, ^{t}Bu), −2.53 (s, BH bridge), −2.63 (s, BH bridge). IR (NaCl plate, cm^{-1}): 3400 (s), 2970 (vs), 2873 (s), 2577 (vs), 2350 (m), 2285 (m), 2072 (m), 1605 (m), 1590 (m), 1495 (s), 1455 (s), 1398 (s), 1363 (vs), 1231 (s), 1215 (s), 1122 (s), 1087 (s), 1039 (s), 955 (s), 888 (s), 875 (m), 856 (w), 760 (m), 742 (s), 713 (s), 610 (s).

Reaction of 3 with HCl·Et_2O. A ~0.2 g sample of **3** and ~0.2 mL of CH_2Cl_2 were added into an NMR tube. The mixture was cooled at −78 °C, and then ~0.25 mL of HCl·Et_2O (1 M) was added. Bubbles were generated and ^{11}B NMR analysis showed the formation of 6-Cl-*nido*-5,7-$C_2B_8H_{11}$.[8] ^{11}B NMR (128.4 MHz, CH_2Cl_2, ppm,): 36.5 (s, 1B), −0.1 (d, 2B), −12.3 (d, 1B), −21.1 (d, 2B), −33.5 (d, 1B), −48.0 (d, 1B).

Computational Methods. The DFT/GIAO/NMR computations employed the Gaussian 03 program.[9] The NMR chemical shifts were calculated at the B3LYP/6-311G* level using the GIAO option within Gaussian 03 and are referenced to $BF_3{\cdot}O(C_2H_5)_2$ using an absolute shielding constant of 102.24 ppm. For the energy calculations, both the ground and transition state geometries were optimized at the B3PW91/6-31G* and/or B3LYP/6-31G* levels. A vibrational frequency analysis was carried out on each optimized geometry with a true minimum (i.e., no imaginary frequencies) found for each ground-state structure. The energies (Supporting Information, Table S1) for the optimized geometries were calculated at the DFT B3PW91/6-31G* and/or B3LYP/6-31G* levels, and with second-order Møller−Plesset perturbation theory (MP2) with a frozen core approximation (i.e., only valence electrons were considered for the electron correlation treatment) in conjunction with the 6-311+G(d,p) basis set. The zero-point vibrational energies were computed and then scaled.[10] All reported MP2 energies are corrected using the scaled zero-point energies.

Results and Discussion

All reactions were carried out under argon in biphasic 1-butyl-3-methylimidazolium chloride (bmimCl)/toluene mixtures at ~120 °C with vigorous stirring to form an emulsion of the two phases.

Hawthorne has previously reported[8] both that reaction of the *arachno*-4,6-$C_2B_7H_{12}^-$ anion with diborane in diethylether produced the *nido*-5,7-$C_2B_8H_{12}$ and *closo*-1,6-$C_2B_8H_{10}$ cage-expanded products and that the *nido*-5,7-$C_2B_8H_{12}$ could then be quantitatively converted at 150 °C to *closo*-1,6-$C_2B_8H_{10}$. Therefore, it was not surprising that when *arachno*-4,6-$C_2B_7H_{13}$ was reacted with trimethylamine borane in bmimCl/toluene at 120 °C, both expansion and dehydrogenation occurred to produce *closo*-1,6-$C_2B_8H_{10}$ (eq 4).[11]

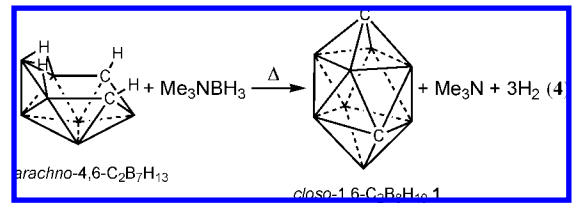

However, when *arachno*-4,6-$C_2B_7H_{13}$ was reacted with dimethylamine borane or *tert*-butylamine borane in bmimCl/toluene, ^{11}B NMR analyses of the toluene layers indicated that another product was formed in addition to *closo*-1,6-$C_2B_8H_{10}$ (eq 5).

$$\textit{arachno}\text{-}4,6\text{-}C_2B_7H_{13} + RR'NHBH_3 \xrightarrow{\Delta,\ -H_2} \underset{(1)}{\textit{closo}\text{-}1,6\text{-}C_2B_8H_{10}} + \underset{\substack{(2)\ R=R'=Me\\(3)\ R=H,\ R'=t\text{-}Bu}}{6\text{-}(RR'N)\text{-}\textit{nido}\text{-}5,7\text{-}C_2B_8H_{11}} \quad (5)$$

The higher volatility of the *closo*-1,6-$C_2B_8H_{10}$ allowed it to be easily removed in vacuo to leave behind the air sensitive 6-(Me_2N)-*nido*-5,7-$C_2B_8H_{11}$ (**2**) and 6-(^{t}BuHN)-*nido*-5,7-$C_2B_8H_{11}$ (**3**) products. The mass spectrum of **2** showed a characteristic eight-boron pattern parent-envelope with the expected cutoff at *m/e* 167, while that of **3** had a diminished parent ion (*m/e* 195) indicating the facile loss of one hydrogen The exact mass determination for **3** on its parent-1 ion (*m/e* 194) was likewise consistent with this proposed fragmentation.

(7) (a) Garrett, P. M.; Smart, J. C.; Ditta, G. S.; Hawthorne, M. F. *Inorg. Chem.* **1969**, *8*, 1907–1910. (b) Tebbe, F. N.; Garrett, P. M.; Hawthorne, M. F. *J. Am. Chem. Soc.* **1968**, *90*, 869–879. (c) Teixidor, F.; Vinas, C.; Rudolph, R. W. *Inorg. Chem.* **1986**, *25*, 3339–3345.

(8) Garrett, P. M.; Ditta, G. S.; Hawthorne, M. F. *J. Am. Chem. Soc.* **1971**, *93*, 1265–1266.

(9) Frisch, M. J.; et al. *Gaussian 03,* revision B.05; Gaussian, Inc.: Pittsburgh, PA, 2003.

(10) Merrick, J. P.; Moran, D.; Radom, L. *J. Phys. Chem. A* **2007**, *111*, 11683–11700.

(11) Only the *endo*-CH and boron-bridging hydrogens are shown in these drawings. Each cage carbon and boron also has one additional terminal hydrogen.

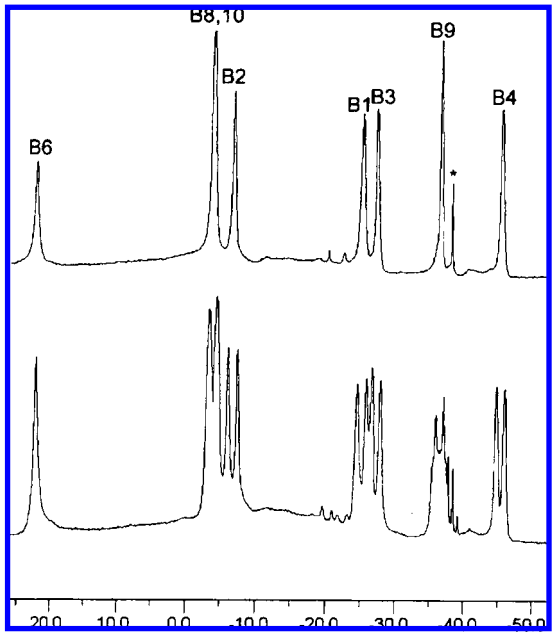

Figure 1. The ^{11}B NMR spectra of 6-(^{t}BuHN)-*nido*-5,7-$C_2B_8H_{11}$ (**3**): (top) ^{1}H-decoupled; (bottom) ^{1}H-coupled; (∗) BH_4^- impurity.

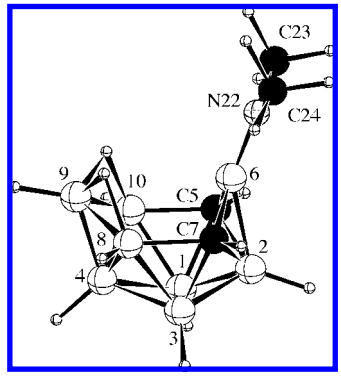

Figure 2. DFT optimized geometries (B3LYP/6-311G*) and selected calculated bond lengths (Å) and bond angles (deg) for 6-(Me_2N)-*nido*-5,7-$C_2B_8H_{11}$ (**2**): C5−B6, 1.588; B6−C7, 1.587; C7−B8, 1.656; B8−B9, 1.821; B9−B10, 1.821; C5−B10, 1.656; B1−B2, 1.726; B2−B3, 1.726; B2−C5, 1.694; B2−C7, 1.694; B2−B6, 1.860; B1−B3, 1.755; B1−B4, 1.790; B1−C5, 1.688; B1−B10, 1.826; B3−B4, 1.791; B3−C7, 1.689; B3−B8, 1.827; B4−B8, 1.822; B4−B9, 1.736; B4−B10, 1.821; B6−N22, 1.398; N22−C23, 1.457; N22−C24, 1.457; C5−B6−N22, 127.9; C7−B6−N22, 127.9; C5−B6−C7, 104.1; B6−N22−C23, 123.4; B6−N22−C24, 123.4; C23−N22−C24, 113.2; B6−C5−B10, 106.8; B6−C7−B8, 106.8; C5−B10−B9, 119.2; C7−B8−B9, 119.2, B2−B6−N22, 146.7.

The ^{11}B NMR spectrum of **2** has a pattern similar to that of the parent *nido*-5,7-$C_2B_8H_{12}$,[8] consisting of six resonances in 1:2:1:2:1:1 ratios suggesting a C_s-symmetric cage structure, while that of **3**, which has two different substituents at N, showed (Figure 1) seven resonances in 1:2:1:1:1:1:1 ratios. In both **2** and **3**, the resonance at lowest field (near 23 ppm) was a singlet, suggesting nitrogen substitution at this site, while a doublet upfield resonance near ca. −37 ppm showed additional triplet fine structure, indicating its coupling to two bridging hydrogens.

DFT/GIAO calculations at the B3LYP/6-311G* level generated the optimized geometries for **2** and **3** shown in Figures 2 and 3. The compounds have the same C_2B_8 cage-framework proposed for the parent *nido*-5,7-$C_2B_8H_{10}$ carborane,[8] where the boron of the amine borane has become inserted between the two carbons of the starting *arachno*-4,6-$C_2B_7H_{13}$ carborane. Consistent with 24 skeletal electron counts, the compounds can be viewed as being based on an 11-vertex polyhedron missing one vertex. As shown in Table 1, there is excellent agreement between the calculated and experimental ^{11}B NMR chemical shifts for these structures. Most significantly, the calculated chemical shifts of the singlet-resonance of the B6-boron with the amine-substituent and that of the B9-boron attached to the two bridge-hydrogens are correctly predicted to be near 23 and −37 ppm, respectively. **2** is also correctly predicted to have the observed 1:2:1:2:1:1 pattern. **3** does not have C_s symmetry owing to the different (^{t}Bu and H) substituents at nitrogen, and the calculations are again in excellent agreement with the experimentally observed 1:2:1:1:1:1:1 pattern, with the intensity-two resonance at −3.8 ppm arising from the overlap of the B8 and B10 resonances that the calculations predict will have almost identical chemical shifts (−4.6 ppm, B8 and −4.8 ppm, B10).

The most unique feature of these compounds concerns the nature of the bonding of the B6 boron to the exopolyhedral amine nitrogen. The length of a covalent B−N single bond is generally near ∼1.5 Å,[12] but the calculations indicate greatly shortened B−N bonds, 1.398 Å for **2** and 1.398 Å for **3**. These

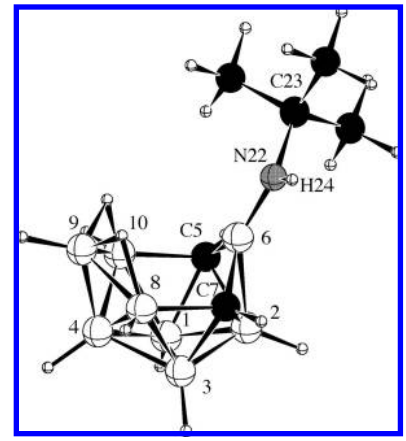

Figure 3. DFT optimized geometries (B3LYP/6-311G*) and selected calculated bond lengths (Å) and bond angles (deg) for 6-(^{t}BuNH)-*nido*-5,7-$C_2B_8H_{11}$ (**3**): C5−B6, 1.582; B6−C7, 1.592; C7−B8, 1.653; B8−B9, 1.820; B9−B10, 1.820; C5−B10, 1.659; B1−B2, 1.724; B2−B3, 1.726; B2−C5, 1.697; B2−C7, 1.693; B2−B6, 1.859; B1−B3, 1.755; B1−B4, 1.790; B1−C5, 1.691; B1−B10, 1.828; B3−B4, 1.789; B3−C7, 1.687; B3−B8, 1.827; B4−B8, 1.822; B4−B9, 1.737; B4−B10, 1.821; B6−N22, 1.398; N22−C23, 1.485; C5−B6−N22, 131.3; C7−B6−N22, 124.5; C5−B6−C7, 104.1; B6−N22−C23, 131.2; B6−N22−H24, 115.9; C23−N22−H24, 112.8; B6−C5−B10, 106.9; B6−C7−B8, 107.2; C5−B10−B9, 119.2; C7−B8−B9, 119.0, B2−B6−N22, 145.7.

Table 1. Comparisons of the Experimental and DFT/GIAO (B3LYP/6-311G*) Calculated ^{11}B NMR Chemical Shifts for 6-(Me_2N)-*nido*-5,7-$C_2B_8H_{11}$ (**2**) and 6-(^{t}BuHN)-*nido*-5,7-$C_2B_8H_{11}$ (**3**)

6-(Me_2N)-*nido*-5,7-$C_2B_8H_{11}$ **2**			6-(^{t}BuHN)-*nido*-5,7-$C_2B_8H_{11}$ **3**		
assign	calcd	expt	assign	calcd	expt
B6	23.4	22.7	B6	22.7	22.5
B8,10	−5.0	−4.0 (2)	B8	−4.6	−3.8 (2)
B2	−6.9	−6.3	B10	−4.8	
B1,3	−24.5	−25.9 (2)	B2	−7.0	−6.5
B9	−38.5	−36.6	B1	−23.4	−25.1
B4	−47.8	−45.2	B3	−25.4	−27.2
			B9	−37.9	−36.4
			B4	−47.6	−45.1

(12) Paetzold, P. *Adv. Inorg. Chem.* **1987**, *31*, 123–170.

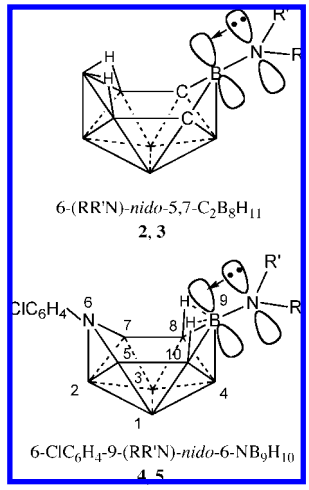

Figure 4. Possible boron−nitrogen π-bonding interactions in 6-(RR′N)-*nido*-5,7-$C_2B_8H_{11}$ (**2** and**3**) and in the previously proposed[14] structure of 6-ClC_6H_4-9-(RR′N)-*nido*-6-NB_9H_{10} (**4** and **5**).[11]

values fall in the range observed for compounds containing boron−nitrogen double bonds, such as in $H_2N{=}BH_2$ (1.391(2) Å),[13] $Me_2B{=}NMe_2$ (1.403(1) Å),[14] $Me_2B{=}NHMe$ (1.397 (2) Å),[15] $(CF_3)_2B{=}NMe_2$ (1.425(18) Å)[16] and $(CF_3)_2B{=}N^iPr_2$ (1.37(1) Å).[17] Likewise, the angles around the nitrogen atoms in **2** (123.4°, 123.4°, 113.2°; sum = 360°) and **3** (115.9°, 131.2°, 112.8°; sum = 359.9°), and the fact that the B6 boron lies in the same plane as the nitrogen and its two substituents, all suggest, as depicted in Figure 4 (top), an sp^2-hybridized nitrogen that is donating its lone pair to a vacant orbital on the B6-boron to form a B=N double bond. The excellent agreement of the chemical shifts for the optimized C_1 structure of **3** with its experimental room temperature ^{11}B NMR spectrum also supports the presence of a B=N bond that is not fastly rotating on the NMR time scale at room temperature in solution. **3** decomposed at higher temperatures.

The availability of an acceptor orbital on the B6 boron of *nido*-5,7-$C_2B_8H_{12}$ was previously demonstrated[8] by its reaction with trimethylamine (eq 6[11]) to produce the 6-Me_3N-*nido*-5,7-$C_2B_8H_{12}$ adduct with the amine bonded to the B6 boron. The amine adduct was then shown to react with HCl to form 6-Cl-*nido*-5,7-$C_2B_8H_{11}$.

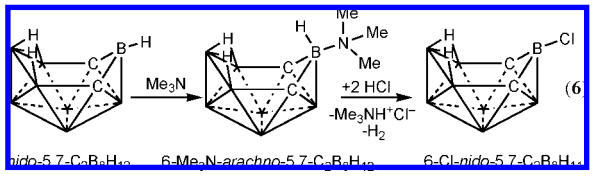

The DFT optimized geometries of *nido*-5,7-$C_2B_8H_{12}$, 6-Me_3N-*arachno*-5,7-$C_2B_8H_{12}$ and 6-Cl-*nido*-5,7-$C_2B_8H_{11}$ are presented in Figure 5. In contrast to the short B=N lengths found in **2**

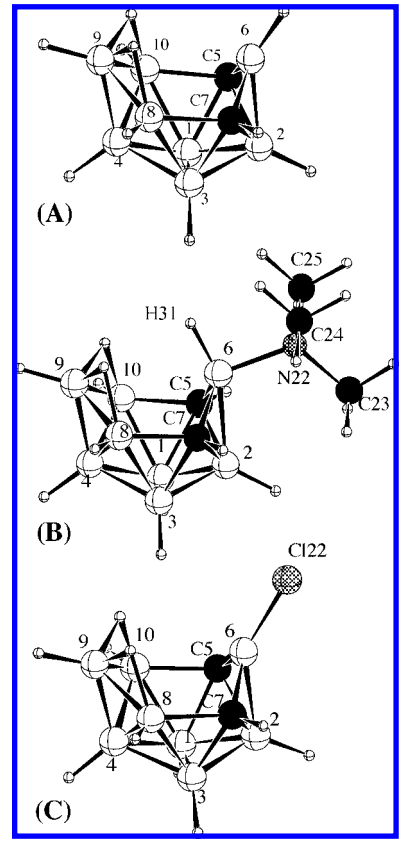

Figure 5. DFT optimized geometries (B3LYP/6-311G*) and selected calculated bond lengths (Å) and bond angles (deg) for (**A**) *nido*-5,7-$C_2B_8H_{12}$, (**B**) *arachno*-6-Me_3N-5,7-$C_2B_8H_{12}$, and (**C**) 6-Cl-*nido*-5,7-$C_2B_8H_{12}$: (**A**) B1−B2, 1.735; B1−B3, 1.767; B1−B4, 1.791; B1−C5, 1.684; B1−B10, 1.827; B2−B3, 1.734; B2−C5, 1.694; B2−B6, 1.816; B2−C7, 1.694; B3−B4, 1.791; B3−C7, 1.684; B3−B8, 1.826; B4−B8, 1.814; B4−B9, 1.735; B4−B10, 1.815; C5−B6, 1.556; B6−C7, 1.556; C7−B8, 1.679; B8−B9, 1.809; B9−B10, 1.810; C5−B10, 1.678; B2−B6−H22, 140.6; C5−B6−H22, 126.5; C7−B6−H22, 126.5; C5−B6−C7, 106.3. (**B**) B1−B2, 1.714; B1−B3, 1.742; B1−B4, 1.782; B1−C5, 1.708; B1−B10, 1.816; B2−B3, 1.714; B2−C5, 1.677; B2−B6, 1.943; B2−C7, 1.678; B3−B4, 1.782; B3−C7, 1.708; B3−B8, 1.816; B4−B8, 1.833; B4−B9, 1.735; B4−B10, 1.834; C5−B6, 1.660; B6−C7, 1.661; C7−B8, 1.640; B8−B9, 1.835; B9−B10, 1.834; C5−B10, 1.640; B6−N22, 1.704; C7−B6−N22, 116.8; C5−B6−N22, 116.9; B2−B6−N22, 106.2; C5−B6−C7, 98.8; N22−B6−H31, 97.8; B6−N22−C23, 119.4; B6−N22−C24, 116.4; B6−N22−C25, 106.4. (**C**) B1−B2, 1.730; B1−B3, 1.767; B1−B4, 1.791; B1−C5, 1.684; B1−B10, 1.827; B2−B3, 1.730; B2−C5, 1.704; B2−B6, 1.830; B2−C7, 1.704; B3−B4, 1.791; B3−C7, 1.684; B3−B8, 1.827; B4−B8, 1.815; B4−B9, 1.734; B4−B10, 1.815; C5−B6, 1.552; B6−B7, 1.552; C7−B8, 1.681; B8−B9, 1.809; B9−B10, 1.809; C5−B10, 1.681, B6−Cl, 1.763; C5−B6−Cl, 126.4; C7−B6−Cl, 126.4; C5−B6−C7, 106.8; B2−B6−Cl, 142.1.

and **3**, the B6−N bond (1.704 Å) in 6-Me_3N-*arachno*-5,7-$C_2B_8H_{12}$ falls in the normal dative boron−nitrogen single bond range.[18] Both *nido*-5,7-$C_2B_8H_{12}$ and 6-Cl-*nido*-5,7-$C_2B_8H_{11}$ have structural features similar to **2** and **3**. For example, in all four compounds the sum of their C5−B6−C7, C5−B6−X and C7−B6−X bond angles indicates a planar coordination of the B6 boron to the C5, C7, and X atoms (**2**, 359.7°; **3**, 359.9° (X = N); *nido*-5,7-$C_2B_8H_{12}$, 359.4° (X = H); 6-Cl-*nido*-5,7-$C_2B_8H_{11}$, 359.7° (X = Cl)). Likewise, the B6−Cl bond length (1.763 Å) in 6-Cl-*nido*-5,7-$C_2B_8H_{11}$ is similar to that found in

(13) Sugie, M.; Takeo, H.; Matsumura, C. *J. Mol. Spectrosc.* **1987**, *123*, 286–292.
(14) Boese, R.; Niederprum, N.; Blaser, D. *Struct. Chem.* **1992**, *3*, 399–406.
(15) Almenningen, A.; Gundersen, G.; Mangerud, M.; Seip, R. *Acta. Chem. Scand. A* **1981**, *35*, 341–357.
(16) Pawelke, G.; Burger, H. *Appl. Organomet. Chem.* **1996**, *10*, 147–174.
(17) (a) Atoji, M.; Lipscomb, W. N. *J. Chem. Phys.* **1957**, *27*, 195. (b) Wagner, T.; Eigendorf, U.; Herberich, G. E.; Englert, U. *Struct. Chem.* **1994**, *5*, 233–237.
(18) (a) Gilbert, T. M. *J. Phys. Chem.* **2004**, *108*, 2550–2554. (b) Ostby, K-A.; Gundersen, G.; Haaland, A.; Noth, H. *Dalton Trans.* **2005**, 2284–2291.

compounds having significant boron−chlorine π-bonding interactions, such as in, BCl_3 (1.75 (2) Å)[17a] and 2-chloro-2-boraindane (1.751 (3) Å)[17b] and is much shorter than the B−Cl single bonds found in, for example H_3NBCl_3, (1.837 (4) average)[19] and BCl_4^- (1.85 (1) average).[20] These common features further support, as originally proposed by Hawthorne,[8] the availability of an acceptor orbital on B6.

As shown in the example in eq 7, aminoboranes can undergo addition reactions, and this reaction has previously been used as a chemical test for the presence of a B=N double bond.[16]

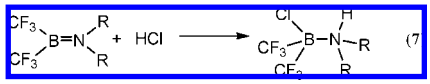

However, when an NMR tube reaction of **3** and $HCl\cdot Et_2O$ in CH_2Cl_2 was carried out at −78 °C, ^{11}B NMR analysis showed that, instead of an addition product, 6-Cl-*nido*-$C_2B_8H_{11}$ was formed. Even in experiments where less than 2 equiv of HCl were added, only unreacted **3** and 6-Cl-*nido*-$C_2B_8H_{11}$ were observed. This result, along with the results of the earlier Hawthorne studies[8] of the reaction of 6-Me_3N-*arachno*-5,7-$C_2B_8H_{12}$ with HCl (eq 6), suggests the reaction sequence shown in eq 8,[11] where following initial HCl addition across the B=N, additional HCl readily protonates the amine inducing elimination of the $R_2NH_2^+Cl^-$ salt.

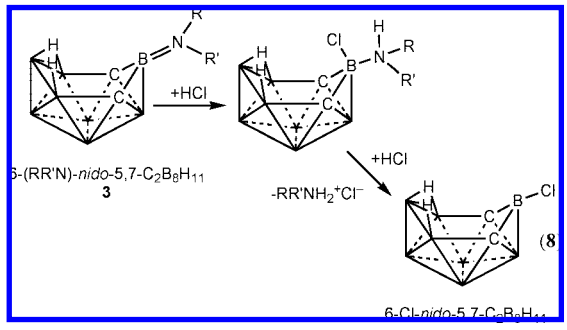

Paetzold[21] had previously proposed that there was also substantial B=N double bond character between the amino-nitrogen and the 9-vertex cage-boron in the 6-ClC_6H_4-9-(RR′N)-*nido*-6-NB_9H_{10} (R/R′ = H/^{t}Bu, Et/Et or ^{i}Pr/^{i}Pr) azaborane clusters shown in Figure 4 (bottom), and that, as a result, these compounds should have structures that are hybrids of *nido/arachno* cage-systems. Since no structural determinations have been reported, we carried out computational studies of two of Paetzold's compounds, 6-ClC_6H_4-9-(^{i}Pr_2N)-*nido*-6-NB_9H_{10} (**4**) and 6-ClC_6H_4-9-(^{t}BuHN)-*nido*-6-NB_9H_{10} (**5**) to allow comparisons of their possible B=N interactions with those in **2** and **3**. The optimized structures of **4** and **5** shown in Figures 6 and 7 both show boron−nitrogen bonding features quite similar to those found in **2** and **3** with the B9−N20 bond lengths for **4** (1.386 Å) and **5** (1.381 Å) again falling in the double-bond range. Likewise, the angles around the N20 nitrogen atom in **4** (120.5°, 115.1°, 124.3°; sum = 359.9°) and **5** (131.2°, 112.6°, 116.1°; sum = 359.9°), and the fact that the B9 boron lies in

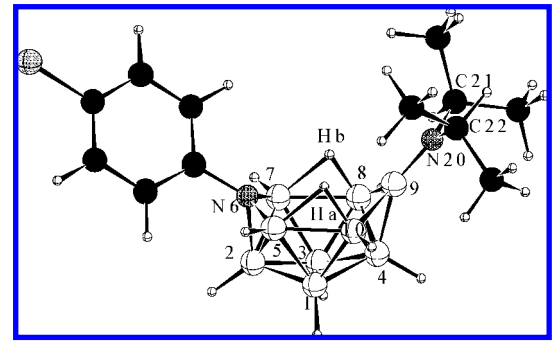

Figure 6. DFT optimized geometries (B3LYP/6-311G*) and selected calculated bond lengths (Å) and bond angles (deg) for 6-ClC_6H_4-9-(^{i}Pr_2N)-*nido*-6-NB_9H_{10} (**4**): B1−B2, 1.757; B1−B3, 1.845; B1−B4, 1.768; B1−B5, 1.774; B1−B10, 1.787; B2−B3, 1.756; B2−B5, 1.859; B2−N6, 1.602; B2−B7, 1.864; B3−B4, 1.771; B3−B7, 1.772; B3−B8, 1.786; B4−B8, 1.772; B4−B9, 1.696; B4−B10, 1.775; B5−N6, 1.531; N6−B7, 1.522; B7−B8, 1.869; B8−B9, 1.838; B9−B10, 1.822; B5−B10, 1.869; B9−N20, 1.386; Hb−B7 1.575, Hb−B8, 1.245; Hb−B9, 2.065; Ha−B5, 1.543; Ha−B10, 1.248; Ha−B9, 2.066; B8−B9−B10, 102.8; B8−B9−N20, 125.6; B10−B9−N20, 130.1; B9−N20−C21, 120.5; C21−N20−C22, 115.1; B9−N20−C22, 124.3; B4−B9−N20, 153.0.

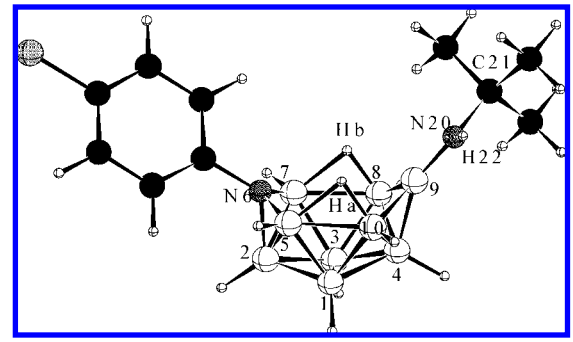

Figure 7. DFT optimized geometries (B3LYP/6-311G*) and selected calculated bond lengths (Å) and bond angles (deg) for 6-ClC_6H_4-9-(^{t}BuHN)-*nido*-6-NB_9H_{10} (**5**): B1−B2, 1.758; B1−B3, 1.849; B1−B4, 1.771; B1−B5, 1.774; B1−B10, 1.786; B2−B3, 1.759; B2−B5, 1.864; B2−N6, 1.599; B2−B7, 1.863; B3−B4, 1.763; B3−B7, 1.777; B3−B8, 1.793; B4−B8, 1.781; B4−B9, 1.692; B4−B10, 1.772; B5−N6, 1.532; N6−B7, 1.524; B7−B8, 1.877; B8−B9, 1.804; B9−B10, 1.827; B5−B10, 1.864; B9−N20, 1.381; Hb−B7, 1.558; Hb−B8, 1.248; Hb−B9, 2.036; Ha−B5, 1.542; Ha−B10, 1.250; Ha−B9, 2.066; B8−B9−B10, 104.2; B8−B9−N20, 131.9; B10−B9−N20, 122.2; B9−N20−C21, 131.2; C21−N20−H22, 112.6; B9−N20−H22, 116.1; B4−B9−N20, 153.5.

the same plane as the nitrogen and its two substituents again indicate an sp^2-hybridized nitrogen that is donating its lone pair to a vacant orbital on the B9-boron to form a B=N double bond. As can also be seen in the Figures, the two bridging-hydrogens that were originally proposed[21a] to be at the B8−B9 and B9−B10 edges in the structure in Figure 4 are instead asymmetrically bonded at the B5−B10 and B7−B8 edges in the optimized structures, being, as also proposed by Paetzold,[21] much closer to the *endo*-positions at the B8 and B10 atoms. The B5−B10 and B7−B8 edges are, in fact, the favored positions for bridging-hydrogens in 10-vertex *arachno*-structures,[22] such as *arachno*-$B_{10}H_{12}^{2-}$[23] and *arachno*-6,9-$C_2B_8H_{14}$.[24]

(19) Avent, A. G.; Hitchcock, P. B.; Lappert, M. F.; Liu, D-S.; Mignani, G.; Richard, C.; Roche, E. *J. Chem. Soc., Chem. Commun.* **1995**, 855–856.
(20) Crespi, A. M.; Shriver, D. F. *Organometallics* **1985**, *4*, 1830–1835.
(21) (a) Roth, A.; Meyer, F.; Paetzold, P. *Collect. Czech. Chem. Commun.* **1997**, *62*, 1299–1309. (b) Paetzold, P. *Eur. J. Inorg. Chem.* **1998**, *2*, 143–154.
(22) Williams, R. E. *Chem. Rev.* **1992**, *92*, 177–207.
(23) Kendall, D. S.; Lipscomb, W. N. *Inorg. Chem.* **1973**, *12*, 546–551.
(24) (a) Stibr, B.; Plesek, J.; Hermanek, S. *Collect. Czech. Chem. Commun.* **1974**, *39*, 1805–1809. (b) Stibr, B.; Plesek, J.; Hermanek, S. *Chem. Ind. (London)* **1972**, 963–964. (c) Wermer, J. R.; Hosmane, N. S.; Alexander, J. J.; Siriwardane, U.; Shore, S. G. *Inorg. Chem.* **1986**, *25*, 4351–4354.

Table 2. Comparisons of the Experimental and DFT/GIAO (B3LYP/6-311G*) Calculated ^{11}B NMR Chemical Shifts for 6-ClC_6H_4-9-(^{i}Pr$_2$N)-*nido*-6-NB_9H_{10} (**4**) and 6-ClC_6H_4-9-(^{t}BuHN)-*nido*-6-NB_9H_{10} (**5**)

6-ClC_6H_4-9-(^{i}Pr$_2$N)-*nido*-6-NB_9H_{10} **4**				6-ClC_6H_4-9-(^{t}BuHN)-*nido*-6-NB_9H_{10} **5**			
assign	calcd	average	expt	assign	calcd	average	expt
B9	42.8	42.8	37.3	B9	42.4	42.4	36.3
B5	3.3	3.6 (2)	9.2 (2)	B5	3.6	3.5 (2)	8.9 (2)
B7	3.8			B7	3.4		
B4	−1.3	−1.3	−6.5	B4	−0.1	−0.1	−7.2
B2	−18.3	−18.3	−23.9	B2	−17.8	−17.8	−24.5
B3	−33.8	−33.0 (2)	−23.1 (2)	B3	−31.0	−33.2 (2)	−23.9 (2)
B1	−32.2			B1	−35.3		
B8	−44.6	−44.9 (2)	−40.1 (2)	B8	−46.4	−44.3 (2)	−39.4 (2)
B10	−45.1			B10	−42.1		

The fact that the bridging hydrogens in **4** and **5** adopt these edges, gives strong support to Paetzold's proposed hybrid *nido*/*arachno* structural formulation arising from the increased cage skeletal electron count resulting from the electron-pair donation of the amino group. From this point of view, **2** and **3** could likewise be considered to have an *arachno* rather than *nido* electron count framework, but in their case, like in the *arachno*-6-R-6,5,7-$C_3B_7H_{11}$ tricarbaboranes[25] and the *arachno*-6-R-6,5,7-$PC_2B_7H_{11}$ phosphacarboranes,[26] the 5 and 7 cage vertices are occupied by carbons, so the bridge hydrogens are prevented from occupying the analogous C5−B10 and C7−B8 edges in these structures.

Like **3**, both **4** and **5** have optimized C_1-symmetric structures, but in contrast to **3**, which also exhibited a C_1 symmetric pattern in its solution ^{11}B NMR spectrum, both **4** and **5** showed 1:2:1:1:2:2 patterns in their spectra suggesting C_s-symmetric structures. Such a C_s pattern could arise if there was fast rotation on the NMR time scale about the B9−N20 bonds (this would also require free rotation about the N20−C22 and N20−C21 bonds in **4**) and, as given in Table 2, when the calculated chemical shifts for the **4** and **5** optimized C_1 geometries are averaged to take into account those borons that would become equivalent in such a process (i.e., B8 with B10; B5 with B7; and B1 with B3), there is fair agreement of these averaged values with the experimentally observed chemical shifts and assignments. Poorest agreement is found for the B1,3 borons that lie below the bridge hydrogens on the B7−B8 and B5−B10 edges, where the calculations predict the resonance to be at higher field (−33 ppm) than was experimentally observed (−23 ppm). But Paetzold had reported[21a] that the ^{1}H−^{11}B COSY spectra of **5** showed an interaction between the bridging-hydrogens and B9 so it is likely that in solution, rather than being only at the B5−B10 and B7−B8 edges, the bridging-hydrogens migrate over the B5−B10−B9 and B7−B8−B9 edges and this could certainly result in shifting the B1,3 resonance to somewhat lower field. In fact, as discussed in the next section, our computational studies of the transition state structures required for B═N rotation in **4** and **5**, showed that when the dative nitrogen π-bond to the B9 boron is broken during the rotation, the bridge hydrogens move to the B8−B9 and B10−B9 edges.

The π-bond disruption energies D_π for the series of R′$_2$B═NR_2 aminoboranes were previously calculated at the DFT B3PW91/6-311++G** level by optimizing models where the relative orientations of the BR′$_2$ and R_2N and fragments were fixed in such a manner that the lone-pair orbital on nitrogen was orthogonal to the vacant 2p-orbital on the boron.[27] The elongation of the B−N bonds, H_2BNH_2 (1.468 Å), H_2BNMe_2 (1.462 Å), Me_2BNH_2 (1.486 Å), and Me_2BNMe_2 (1.486 Å), and the conversion to a pyramidal geometry at nitrogen observed in the optimized rotated-structures were consistent with disruption of the dative π-bond. The energy difference between the two configurations shown in eq 9 then provided a measure of dative π-bond strength and the barrier for internal rotation: H_2B═NH_2 (32.5 kcal/mol), H_2B═NMe_2 (34.5 kcal/mol), Me_2B═NH_2 (27.2 kcal/mol), and Me_2B═NMe_2 (25.6 kcal/mol).

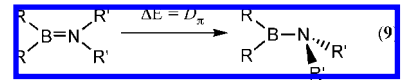

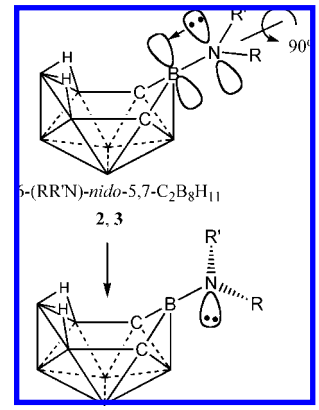

Figure 8. Schematic diagram showing that in **2** or **3**, a 90° rotation of the R_2N group about the B−N bond axis leads to disruption of the dative N→B π-donation. The resulting localization of the lone pair at the nitrogen requires the conversion to a pyramidal configuration for the amine.[11]

Analogous calculations were performed on **2** and **3** by optimizing the structures generated by rotating, as schematically depicted in Figure 8, their R_2N groups by 90°. Similar results were obtained using either the B3PW91 and B3LYP functionals, so only the bond distance and angle values for the B3LYP calculations are given. For **3**, two transition state structures are possible depending upon whether the rotation places the R group in the up (**TS3a**) or down (**TS3b**) positions at the nitrogen. Geometry optimization of the **2** and **3** rotated structures then yielded the transition state structures given in Figures 9 and 10, with the imaginary vibrational frequencies for these structures corresponding to rotation about the B−N bond axis. Consistent with the disruption of the boron nitrogen π-bond, the B6−N bonds of **TS2** (1.459 Å), **TS3a** (1.463 Å), and **TS3b** (1.459 Å) lengthen, and the sum of the angles around the nitrogens indicates that in each case the BNR_2 unit is no longer planar, **TS2** (115.2°, 115.4°, 112.0°; sum = 342.6°), **TS3a** (124.6°, 109.4°, 108.8°; sum = 342.8°) and **TS3b** (125.7°, 109.7°, 108.8°; sum = 342.6°). This suggests, as depicted in Figure 8, the localization of the lone-pair of electrons on the pyramidal amino-nitrogen. The B6−B2 distances in**TS2** (1.824 Å), **TS3a** (1.821 Å), and **TS3b** (1.837 Å) are significantly shortened relative to their values in **2** (1.860 Å) and **3** (1.859 Å) also suggesting that the decrease in the B6−N bonding interaction in the transition state structures enables an increase

(25) Su, K.; Carroll, P. J.; Sneddon, L. G. *J. Am. Chem. Soc.* **1993**, *115*, 10004–10017.
(26) Hong, D.; Rathmill, S. E.; Carroll, P. J.; Sneddon, L. G. *J. Am. Chem. Soc.* **2003**, *125*, 16058–16073.
(27) Ostby, K.-A.; Haaland, A.; Gundersen, G.; Noth, H. *Organometallics* **2005**, *24*, 5318–5328.

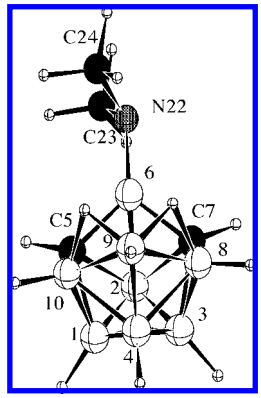

Figure 9. DFT optimized geometry (B3LYP/6-31G*) for the transition state structure **TS2** obtained by a 90° rotation of the Me_2N group about the B−N bond axis of 6-(Me_2N)-*nido*-5,7-$C_2B_8H_{11}$ (**2**). Selected calculated bond lengths (Å) and bond angles (deg): B1−B2, 1.735; B1−B3, 1.773; B1−B4, 1.791; B1−C5, 1.678; B1−B10, 1.822; B2−B3, 1.735; B2−C5, 1.690; B2−B6, 1.824; B2−C7, 1.692; B3−B4, 1.793; B3−C7, 1.676; B3−B8, 1.823; B4−B8, 1.814; B4−B9, 1.738; B4−B10, 1.816; C5−B6, 1.583; B6−B7, 1.574; B7−B8, 1.673; B8−B9, 1.814; B9−B10, 1.817; C5−B10, 1.673; B6−N22, 1.459; N22−C23, 1.462; N22−C24, 1.462; C5−B6−C7, 104.6; C5−B6−N22, 128.5; C7−B6−N22, 126.3; B6−N22−C23, 115.4; B6−N22−C24, 115.2; C23−N22−C24, 112.0; B2−B6−N22, 140.8.

in B6 bonding with the B2 atom that is in a near *trans* position relative to the nitrogen.

Optimization of the structures obtained by a 90° rotation of the $R_2N{=}B$ units of compounds **4** and **5** yielded the transition state structures **TS4** and **TS5a** and **TS5b** shown in Figure 11. The structures have lengthened B9−N20 bonds, **TS4** (1.433 Å), **TS5a** (1.436 Å), and **TS5b** (1.436 Å), again consistent with the disruption of the boron nitrogen π-bond, but the extent of elongation in significantly less than found for **TS2**, **TS3a**, and **TS3b**. Likewise, the sum of the angles around the N20 nitrogen in **TS5a** and **TS5b** indicate that the BNR_2 units are less pyramidal, **TS5a** (116.0°, 128.4°, 111.9°; sum = 356.3°) and **TS5b** (113.2°, 127.9°, 112.3°; sum = 353.4°), than in **TS2**, **TS3a**, and **TS3b**. Surprisingly, even with its elongated B−N bond, the BNR_2 unit in **TS4** (123.0°, 119.1°, 117.9°; sum = 360.0°) remained planar, most likely, as illustrated in Figure 11, because of the large steric interactions of the ^{i}Pr groups. Of perhaps most interest is the fact that the bridging-hydrogens that were at the B5−B10 and B7−B8 edges in the ground state **4** and **5** structures moved to the B8−B9 and B10−B9 edges in the **TS4** and **TS5** structures. This difference again strongly supports Paetzold's hybrid *nido/arachno* formulation of these compounds. Thus, in the ground-state structures, the dative nitrogen π-bond donates two electrons to give each cluster an *arachno* 26 skeletal-electron count thereby causing the two bridging-hydrogens to favor the B5−B10 and B7−B8 edges. But, in the transition state structures, the π-bond is broken, the skeletal electron count is reduced by two, and the two bridging-hydrogens accordingly move to the B8−B9 and B10−B9 edges that are their favored positions in 10-vertex *nido* structures.

The calculated B−N dative π-bond disruption energies obtained from the energy differences calculated at either the DFT or MP2 levels between the ground and transition state structures of **2** (D_π = **Δ2/TS2** = 20.3 (B3LYP); 20.3 (B3PW91); 20.4 kcal/mol (MP2)) and **3** (D_π = **Δ3/TS3a** = 18.8 (B3LYP); 18.3 (B3PW91); 18.4 kcal/mol (MP2)); D_π = **Δ3/TS3b** = 18.6 (B3LYP); 18.8 (B3PW91); 18.9 kcal/mol (MP2)); **4** (D_π = **Δ4/TS4** = 9.4 kcal/mol (B3LYP)) and **5** (D_π = **Δ5/TS5a** = 10.7 kcal/mol (B3LYP); D_π = **Δ5/TS5b** = 9.0 kcal/mol; (B3LYP))

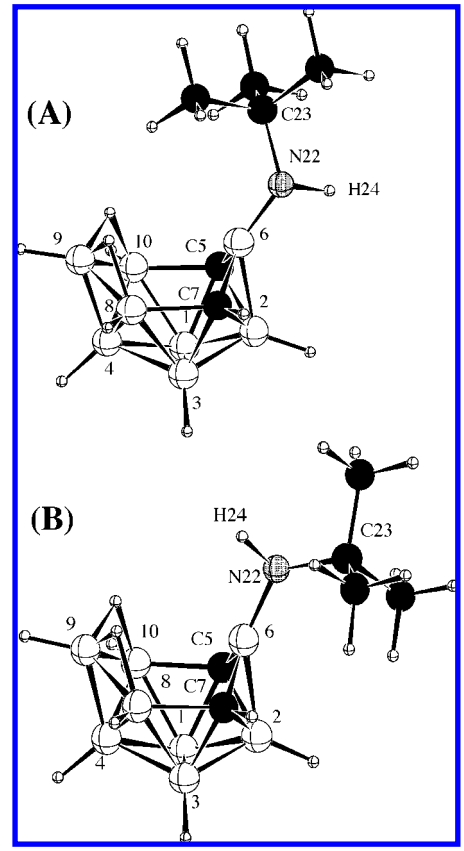

Figure 10. DFT optimized geometries (B3LYP/6-31G*) for the transition state structures **TS3a** and **TS3b** obtained by a 90° rotation of the ^{t}BuNH group about the B−N bond axis of 6-(^{t}BuNH)-*nido*-5,7-$C_2B_8H_{11}$ (**3**). Selected calculated bond lengths (Å) and bond angles (deg): (a) (**TS3a**) B1−B2, 1.733; B1−B3, 1.773; B1−B4, 1.788; B1−C5, 1.683; B1−B10, 1.819; B2−B3, 1.733; B2−C5, 1.692; B2−B6, 1.821; B2−C7, 1.691; B3−B4, 1.791; B3−C7, 1.678; B3−B8, 1.820; B4−B8, 1.819; B4−B9, 1.733; B4−B10, 1.817; C5−B6, 1.584; B6−C7, 1.579; C7−B8, 1.676; B8−B9, 1.813; B9−B10, 1.815; C5−B10, 1.678; B6−N22, 1.463; C5−B6−N22, 129.8; C7−B6−N22, 124.5; C5−B6−C7, 104.0; B6−N22−C23, 124.6; B6−N22−H24, 109.4; C23−N22−H24, 108.8; B2−B6−N22 135.5. (b) (**TS3b**) B1−B2, 1.738; B1−B3, 1.770; B1−B4, 1.794; B1−C5, 1.673; B1−B10, 1.824; B2−B3, 1.738; B2−C5, 1.684; B2−B6, 1.837; B2−C7, 1.687; B3−B4, 1.793; B3−C7, 1.676; B3−B8, 1.823; B4−B8, 1.812; B4−B9, 1.741; B4−B10, 1.812; C5−B6, 1.581; B6−C7, 1.585; C7−B8, 1.669; B8−B9, 1.819; B9−B10, 1.817; C5−B10, 1.669; B6−N22, 1.459; N22−C23, 1.487; C5−B6−N22, 124.8; C7−B6−N22, 131.0; C5−B6−C7, 104.2; B6−N22−C23, 125.7; B6−N22−H24, 109.7; C23−N22−H24, 108.8; B2−B6−N22, 146.9.

are substantially lower that those of the $R_2B{=}NR'_2$ compounds discussed above (∼25 to 35 kcal/mol). These results are consistent with the fact that, unlike in the $R_2B{=}NR'_2$ compounds, where the acceptor orbitals on the planar sp^2-hybridized borons are completely available for nitrogen π-bonding, the B6 boron in **2** and **3** and the B9 boron in **4** and **5** have, in addition to bonding to the nitrogen of their NR_2 groups, competing bonding interactions with the three other atoms (B6 with C5, C7 and B2 in **2** and **3**; B9 with B8, B10, and B4 in **4** and **5**). The higher D_π energies found for **2** and **3** relative to those of **4** and **5** are likewise consistent with the fact that the experimentally observed ^{11}B NMR spectra show that in solution at room temperature **3** has C_1 symmetry (i.e., the B=N bond is not rotating fast on the NMR time scale), while **4** and **5** have apparent C_s symmetry.[21]

The exact role of the bmimCl ionic liquid in promoting the reaction of the amine boranes with *arachno*-4,6-$C_2B_7H_{13}$ has

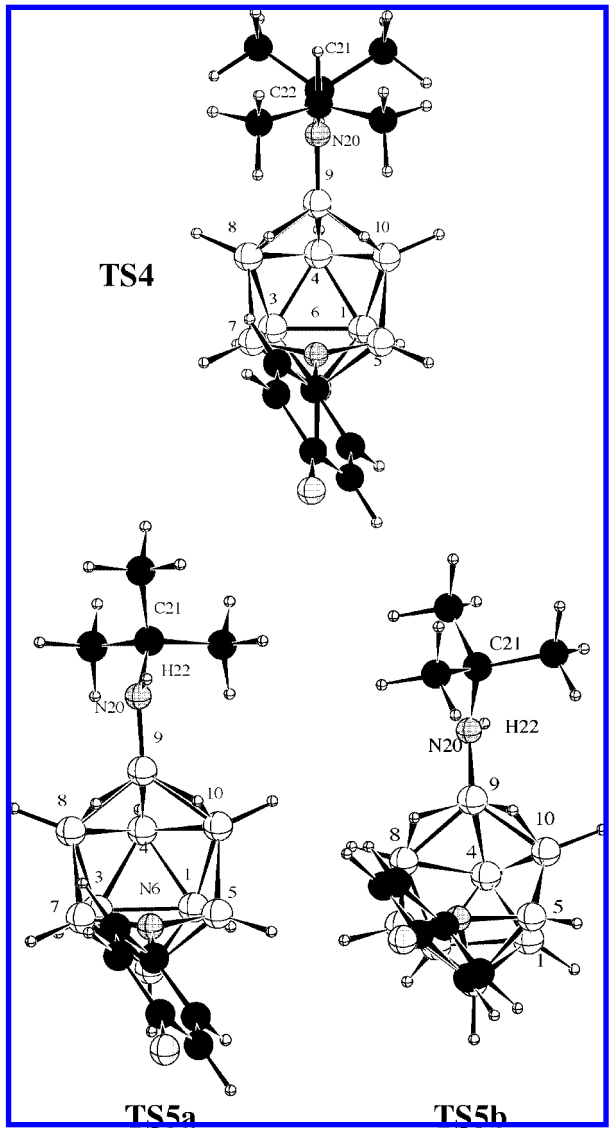

Figure 11. **(a)** DFT optimized (B3LYP/6−31G*) transition state structure **TS4** obtained by a 90° rotation of the $^{i}Pr_2N$ group about the B−N bond axis of 6-ClC_6H_4-9-($^{i}Pr_2N$)-*nido*-6-NB_9H_{10} (**4**). **(b)** DFT optimized (B3LYP/6-31G*) transition state structures **TS5a** and **TS5b** obtained by 90° rotations of the ^{t}BuNH group about the B−N bond axis of 6-ClC_6H_4-9-(^{t}BuHN)-*nido*-6-NB_9H_{10} (**5**). Selected calculated bond lengths (Å) and bond angles (deg): (**TS4**) B1−B2, 1.760; B1−B3, 1.837; B1−B4, 1.806; B1−B5, 1.732; B1−B10, 1.761; B2−B3, 1.762; B2−B5, 1.802; B2−N6, 1.663; B2−B7, 1.805; B3−B4, 1.803; B3−B7, 1.733; B3−B8, 1.760; B4−B8, 1.787; B4−B9, 1.735; B4−B10, 1.785; B5−N6, 1.509; N6−B7, 1.506; B7−B8, 1.934; B8−B9, 1.809; B9−B10, 1.806; B5−B10, 1.932; B9−N20, 1.433; B8−B9−B10, 102.4; B8−B9−N20, 128.5; B10−B9−N20, 128.6; B9−N20−C21, 119.1; C21−N20−C22, 117.9; B9−N20−C22, 123.0; B4−B9−N20, 135.0. (**TS5a**) B1−B2, 1.760; B1−B3, 1.837; B1−B4, 1.809; B1−B5, 1.733; B1−B10, 1.761; B2−B3, 1.761; B2−B5, 1.804; B2−N6, 1.664; B2−B7, 1.805; B3−B4, 1.805; B3−B7, 1.733; B3−B8, 1.760; B4−B8, 1.788; B4−B9, 1.729; B4−B10, 1.788; B5−N6, 1.507; N6−B7, 1.505; B7−B8, 1.932; B8−B9, 1.802; B9−B10, 1.816; B5−B10, 1.930; B9−N20, 1.436; Hb-B8, 1.277; Hb-B9, 1.425; Ha-B10, 1.266; Ha-B9, 1.458; B8−B9−B10, 102.4; B8−B9−N20, 127.2; B10−B9−N20, 130.2; B9−N20−C21, 128.4; C21−N20−H22, 111.9; B9−N20−H22, 116.0; B4−B9−N20, 138.0. (**TS5b**) B1−B2, 1.758; B1−B3, 1.834; B1−B4, 1.807; B1−B5, 1.732; B1−B10, 1.763; B2−B3, 1.765; B2−B5, 1.801; B2−N6, 1.663; B2−B7, 1.807; B3−B4, 1.804; B3−B7, 1.734; B3−B8, 1.760; B4−B8, 1.787; B4−B9, 1.729; B4−B10, 1.786; B5−N6, 1.510; N6−B7, 1.504; B7−B8, 1.935; B8−B9, 1.799; B9−B10, 1.802; B5−B10, 1.926; B9−N20, 1.436; Hb-B8, 1.275; Hb-B9, 1.427; Ha-B10, 1.280; Ha-B9, 1.419; B8−B9−B10, 102.9; B8−B9−N20, 125.9; B10−B9−N20, 130.0; B9−N20−C21, 127.9; C21−N20−H22, 112.3; B9−N20−H22, 113.2; B4−B9−N20, 132.0.

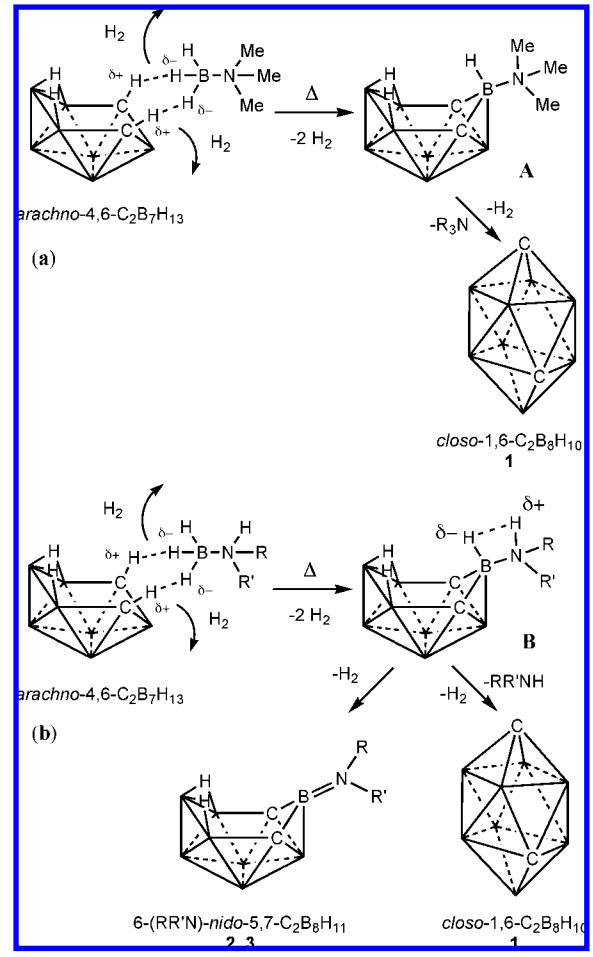

Figure 12. Possible pathways for the reactions of *arachno*-4,6-$C_2B_7H_{13}$ with amine boranes.[11]

not been determined, but no reaction was observed to occur in refluxing toluene in the absence of bmimCl. We have previously shown[1c] that ionic liquids promote the formation of polyaminoborane polymers from ammonia borane by activating a H_2-elimination process involving reaction of the ammonia borane hydridic B−H and protonic N−H hydrogens. The *endo*-hydrogens on the 4,6-carbons of *arachno*-4,6-$C_2B_7H_{13}$ are known to be strongly acidic,[28] while the B−H hydrogens of the amine boranes are hydridic. Therefore, the reaction of the carborane with the amine boranes probably proceeds via the insertion of a H_3BNR_2H unit across the two endo positions of the *arachno*-4,6-$C_2B_7H_{13}$ framework with elimination of 2 H_2. Ionic liquids have been shown to stabilize polar transition states and intermediates,[29] thus, the bmimCl may be simply providing a highly polar medium that promotes the initially required $C-H^{+}\cdots H^{-}-B$ interaction (Figure 12). For the trimethylamine borane reaction, (Figure 12a), once intermediate **A** is formed it

(28) (a) Tebbe, F. N.; Garrett, P. M.; Hawthorne, M. F. *J. Am. Chem. Soc.* **1966**, *88*, 609–608. (b) Tebbe, F. N.; Garrett, P. M.; Hawthorne, M. F. *J. Am. Chem. Soc.* **1968**, *90*, 869–879.

(29) (a) For general reviews of reactions in ionic liquids, see: *Ionic Liquids in Synthesis*; Wassersheid, P., Welton, T., Eds.; Wiley-VCH: Weinheim, Germany, 2003. (b) Dyson, P. J. *Appl. Organomet. Chem.* **2002**, *16*, 495–500. (c) Zhao, H.; Malhotra, S. V. *Aldrich Chimica Acta* **2002**, *35*, 75–83. (d) Sheldon, R. *Chem. Commun.* **2001**, 2399–2407. (e) Wasserscheid, P.; Keim, W. *Angew. Chem., Int. Ed.* **2002**, *39*, 3772–3789. (f) Dupont, J.; de Souza, R. F.; Suarez, P. A. Z. *Chem. Rev.* **2002**, *102*, 3667–3692.

could further react with cage H_2 elimination and Me_3N dissociation to produce *closo*-1,6-$C_2B_8H_{10}$. But for the primary and secondary amine borane reactions, once intermediate **B** is formed there are two different possibilities (Figure 12b) for further reaction: (1) as with the trimethyamine borane, cage H_2 elimination and R_2NH dissociation to form *closo*-1,6-$C_2B_8H_{10}$, or (2) H_2 elimination by reaction of a hydridic hydrogen on boron and a protonic hydrogen on nitrogen to form the B═N double bond observed in **2** and **3**. Regardless of the exact mechanism of these reactions, the results presented herein again clearly illustrate the unique activating effect that ionic liquids can have on polyborane reactions, and further suggest that ionic liquids may provide similar advantages for an even wider array of polyborane transformations. We are currently exploring these possibilities.

Acknowledgment. We thank the National Science Foundation for the support of this project. We also greatly appreciate and thank Mr. Chang Won Yoon for his advice and assistance on computations.

Supporting Information Available: Complete ref 9; tables listing Cartesian coordinates for DFT-optimized geometries and their DFT and MP2 calculated energies. This material is available free of charge via the Internet at http://pubs.acs.org.

JA803297B